Schizophrenia Bulletin
https://doi.org/10.1093/schbul/sbae103

Altered Use of Context During Visual Perception in Psychotic Psychopathology: A Neurophysiological Investigation of Tuned and Untuned Suppression During Contrast Perception

Samuel D. Klein[1,], Collin D. Teich[3], Victor J. Pokorny[1,], Eric Rawls[3], Cheryl A. Olman[1], and Scott R. Sponheim[*,2,3,]

[1]Department of Psychology, University of Minnesota-Twin Cities, Minneapolis, MN, USA; [2]Minneapolis Veterans Affairs Health Care System, Minneapolis, MN, USA; [3]Department of Psychiatry, University of Minnesota Medical School, Minneapolis, MN, USA

[*]To whom correspondence should be addressed; 1 Veterans Drive, Minneapolis, MN 55417, USA; tel: (612) 467-3916, fax: 1-612-626-2079, e-mail: sponh001@umn.edu

***Background and Hypothesis*: The human visual system streamlines visual processing by suppressing responses to textures that are similar to their surrounding context. Surround suppression is weaker in individuals with schizophrenia (ISZ); this altered use of visuospatial context may relate to the characteristic visual distortions they experience. *Study Design*: To understand atypical surround suppression in psychotic psychopathology, we investigated neurophysiological responses in ISZ, healthy controls (HC), individuals with bipolar disorder (IBP), and first-degree relatives (ISZR/IBPR). Participants performed a contrast judgment task on a circular target with annular surrounds, with concurrent electroencephalography. Orientation-independent (untuned) suppression was estimated from responses to central targets with orthogonal surrounds; the orientation-dependence of suppression was estimated by fitting an exponential function to the increase in suppression as surrounds became more aligned with the center. *Results*: ISZ exhibited weakened untuned suppression coupled with enhanced orientation-dependence of suppression. The N1 visual evoked potential was associated with the orientation-dependence of suppression, with ISZ and ISZR (but not IBP or IBPR) showing enhanced orientation-dependence of the N1. Collapsed across orientation conditions, the N1 for ISZ lacked asymmetry toward the right hemisphere; this reduction in N1 asymmetry was associated with reduced *untuned* suppression, real-world perceptual anomalies, and psychotic psychopathology. The overall amplitude of the N1 was reduced in ISZ and IBP. *Conclusions*: Key measures of symptomatology for ISZ are associated with reductions in untuned suppression. Increased sensitivity for ISZ to the relative orientation of suppressive surrounds is reflected in the N1 VEP, which is commonly associated with higher-level visual functions such as allocation of spatial attention or scene segmentation.**

Key words: event-related potentials/surround suppression /schizophrenia/severe mental illness/gain control/current source density

Introduction

Surround suppression occurs when a visual response to a central stimulus (ie, center) is reduced in the presence of a surrounding stimulus (ie, surround).[1,2] This contextual effect contributes to visual functions that are important to navigate and explore the visual world including object boundary detection, figure-ground segmentation, and contour integration.[3–6] Alterations in suppression mechanisms have been linked to core aspects of pathophysiology in individuals with schizophrenia (ISZ),[7] namely visual distortions.[8] Indeed, numerous studies have demonstrated reduced surround suppression in ISZ.[9–11]

Perceptual orientation-dependent surround suppression (ODSS) occurs when the perceived contrast of the center is most strongly reduced when the surround elements are aligned with the center (ie, iso-orientation, surround elements parallel to center)[2]; ODSS is weakest at cross-orientation (ie, surround elements orthogonal to center).[12,13] The suppressive effect of the surround results from a combination of orientation-sensitive (ie, tuned) and -insensitive (ie, untuned) suppression mechanisms.[14–16] We recognize that both tuned and untuned suppression effects, while observed as a single behavioral phenomenon, are likely each a mixture of multiple factors. For example, figure-ground segmentation can be modeled as an (essentially) binary feedback mechanism that gates orientation-tuned suppression.[17] Accordingly, the resulting orientation-sensitive modulation of neural response is a mixture of tuned and untuned neural mechanisms. Here, we use the terms "tuned suppression"

and "untuned suppression" because they have the most straight-forward mapping onto what we observed in the behavioral and EEG data.

Previous work from our laboratory demonstrated that ISZ, their first-degree relatives (ISZR), and individuals with bipolar disorder (IBP) exhibit weakened untuned suppression, with ISZ having the greatest reductions compared to healthy controls (HC).[18,19] This reflected a reduced influence of the surround to suppress the perceived contrast of the target stimulus (ie, central grating with surround), irrespective of orientation. ISZ exhibited atypical tuned suppression, reflecting greater orientation sensitivity in the suppression of perceived target contrast.[18] Notably, this effect was moderated by visual acuity: differences in tuned suppression between ISZ and HC were greatest when acuity was poor. The reduced influence of the surround in ISZ is consistent with the diminished use of visual context to modulate perception[20] and extract meaning from visual scenes,[21] thereby creating the potential for visual distortions and hallucinations.[8]

Investigating the timing of neural events during ODSS can yield insights into the neurophysiological correlates of the altered use of visual context in psychotic psychopathology.[22] For example, the early suppression of primary visual cortex (V1) activity to parallel surrounds (~61 ms compared to ~52 ms to center) implicates rapid feedback from extrastriate cortices (V2/V3), rather than slower horizontal propagation from lateral connections in V1.[23] In human electroencephalography (EEG), surround suppression is observable in early visual evoked potentials (VEP). Evidence suggests that the C1 [~50 ms] results from low-level feedforward activity in geniculocortical pathways (ie, lateral geniculate nucleus [LGN] to V1), and may reflect a neural correlate of untuned suppression.[24–26] Similarly, the P1 [50–140 ms] results from early visual cortical responses in extrastriate cortices,[27–29] which may relate to broadly orientation-tuned mechanisms mediated by perceptual grouping processes.[27,28] Finally, the posterior N1 [120–225 ms], an index of visual discrimination,[30] exhibits orientation-selective suppression consistent with a tuned suppression mechanism.[22,31] Accordingly, it may reflect a neurophysiological correlate of feedback or recurrent modulation of V1 responses (eg, from V4, or lateral occipital cortex)[22,32]; the timing of this component (100–200 ms) would also be consistent with V1 intrinsic suppression mechanism.[14,24,25,33]

Despite its relevance to gain control mechanisms in ISZ,[9,34] no studies have examined the neurophysiological correlates of atypical ODSS during contrast perception in ISZ. The present study sought to address this gap by testing how alterations in early visual neural functions relate to atypical suppression mechanisms in ISZ, ISZR, HC, IBP, and first-degree relatives of IBP (IBPR; total $N = 128$), drawn from the same transdiagnostic sample as our previous work.[18,19] We hypothesized that ISZ would exhibit attenuated responses in the P1 and N1 due to weakened untuned and tuned suppression mechanisms reflecting altered neural activity in extrastriate cortices.[28,35,36] Furthermore, we hypothesized that IBP and ISZR would exhibit intermediate reductions,[18,19] indicative of atypical neurophysiological functions that cut across traditional psychiatric diagnoses and mark genetic liability for psychosis.[37–39] We applied a surface Laplacian transformation to enhance the spatial resolution of VEP,[40] and test whether hemispheric asymmetries in the N1 linked to maintaining attention across hemifields were related to disrupted suppression mechanisms.[41–43] Accordingly, the goals of the present study were 2-fold: (1) characterize the neural correlates of atypical suppression mechanisms during contrast perception in ISZ; and (2) test whether alterations in these neurophysiological dynamics relate to genetic liability for psychosis, and/or reflect a transdiagnostic process related to dimensional aspects of psychotic psychopathology.

Methods

Participants

Individuals with psychotic psychopathology were recruited from Minneapolis Veterans Affairs Health Care System outpatient clinics, community support programs for the mentally ill, and county mental health clinics. Exclusion criteria included: English as a second language, age >60 years, IQ <70, substance dependence within the past 6 months, substance abuse within 2 weeks of testing, head injury with skull fracture or substantial loss of consciousness, electroconvulsive therapy, amblyopia untreated before 18, epilepsy, stroke, or other neurological conditions. Additional exclusion criteria for HC included a significant family history of psychotic psychopathology. Additional recruitment details can be found in recent work by Longenecker et al,[38] and in supplementary materials. Participant demographic information, and other sample characteristics, are presented in table 1.

ODSS Task[18]

We used a contrast-matched ODSS task to examine the effects of visual context on contrast perception. The task is described in full detail in our recent work that modeled surround suppression in the same transdiagnostic sample ($N = 138$).[18] Briefly, a single trial of the task consisted of the simultaneous presentation of a reference circular grating without a surround in 1 hemifield, and a target circular grating (ie, center) with a surrounding annulus (ie, surround) randomly set to 1 of 5 possible relative orientations (0°, 20°, 45°, 70°, and 90°). Participants also viewed a "no surround" condition in which only the reference and target circular grating were presented. Participants responded with a 2-button button box to indicate whether the circular patch in left or right visual hemifields appeared to have higher contrast. Targets

Table 1. Participant Demographics (Total N = 128)

Index	ISZ (N = 28)	ISZR (N = 25)	HC (N = 26)	IBPR (N = 19)	IBP (N = 30)	Test Statistic	Post Hoc Contrasts
Education (years)	13.4 (1.6)	14.89 (2.1)	15.85 (1.4)	15.00 (2.0)	15.17 (2.3)	F = 7.05 , P < .001	ISZ < IBP, HC ISZR, IBPR
Age (years)	46.4 (9.3)	47.5 (8.9)	46.50 (9.5)	40.05 (12.2)	47.43 (10.1)	F = 2.05 , P = .09	—
Percent female (%)	32%	60%	46%	53%	36%	χ^2 = 6.81, P = .15	—
Estimated IQ (WAIS-III)	100.1 (13.3)	106.9 (17.9)	114.6 (13.4)	109.7 (16.4)	101.9 (12.7)	F = 4.07, P < .01	ISZ, IBP < HC
Overall symptomatology (BPRS Total)	40.70 (9.2)	31.52 (8.2)	26.12(2.4)	32.32 (7.9)	37.31 (9.7)	F = 13.0, P < .001	ISZ, IBP > ISZR, IBPR > HC
Positive symptoms (SAPS)	5.25 (3.7)	—	—	—	1.69 (2.3)	t = −4.3 , P < .001	ISZ > IBP
Negative symptoms (SANS)	5.5 (3.0)	—	—	—	4.03 (2.6)	t = −2.03 , P < .01	ISZ > IBP
Psychoticism (PID-5)	1.01 (0.7)	0.36 (0.4)	0.18 (0.18)	0.30 (0.5)	0.83 (0.6)	F = 12.11, P < .001	ISZ, IBP > HC, ISZR, IBPR
Perceptual modulation (SGI)	27.17 (15.3)	16.48 (13.9)	7.72 (8.3)	13.44 (15.8)	27.17 (15.3)	F = 8.87, P < .001	ISZ, IBP < ISZR, IBPR < HC
Visual acuity (LogMAR)	0.15 (0.1)	0.10 (0.1)	0.07 (0.1)	0.04 (0.1)	0.134 (0.1)	F = 3.89, P = .04	—
Orientation Dependent Surround Suppression (ODSS): Behavioral Results							
Contrast differrence (%): 0°	−7.62 (6.4)	−6.73 (3.1)	−8.68 (4.9)	−9.32 (6.7)	−7.38 (5.7)	F = 0.82, P = .51	—
Contrast differrence (%): 90°	−1.59 (4.8)	−2.92 (4.1)	−4.95 (4.3)	−6.35 (5.0)	−2.94 (4.8)	F = 3.87, P < .001	ISZ < HC, IBPR
Width *(w)*	96.15 (77.6)	96.44 (81.3)	78.79 (78.91)	85.11 (81.9)	67.49 (70.51)	F = 0.63, P = .64	—
Magnitude (M)	−9.92 (6.1)	−6.21 (4.5)	−7.63 (5.5)	−5.1 (3.6)	−7.66 (5.2)	F = 2.90, P = .03	ISZ < HC[a]
Offset (o)	1.87 (5.9)	−1.02 (4.2)	−2.14 (4.6)	−4.61 (6.3)	−0.84 (5.7)	F = 3.67, P < .01	ISZ < HC, IBPR
Orientation Dependent Surround Suppression (ODSS): N1 Results							
N1 (μV/cm^2): 0°	−6.65 (4.6)	−11.38 (5.3)	−11.85 (6.8)	−8.79 (4.3)	−9.56 (7.6)	F = 3.27, P = .01	ISZ < HC, ISZR
N1 (μV/cm^2): 90°	−10.26 (5.7)	−14.81 (5.8)	−13.08 (7.5)	−11.99 (4.5)	−10.87 (8.7)	F = 2.03, P = .09	—
Width (w_{N1})	91.47 (83.3)	97.5 (82.2)	73.01 (82.8)	72.02 (81.8)	92.09 (78.4)	F = 0.58, P = .67	—
Magnitude (M_{N1})	−8.15 (6.3)	−6.51 (4.3)	−2.09 (5.3)	−3.96 (3.5)	−3.82 (5.24)	F = 2.86, P = .03	ISZ < HC
Offset (o_{N1})	14.37 (9.1)	17.6 (8.0)	13.81 (9.0)	12.44 (4.9)	12.86 (9.9)	F = 1.37, P = .21	—

Note: Data represent mean (standard deviation), unless otherwise noted. ISZ, individuals with schizophrenia; ISZR, first-degree relatives of ISZ; HC, healthy controls; IBPR, first-degree relatives of IBP; IBP, individuals with bipolar disorder; SAPS/SANS, Scale for the Assessment of Positive/ Negative Symptoms; WAIS-III, Wechsler Adult Intelligence Scale, 3rd edition; IBPRS, 24-item brief psychiatric Rating Scale; PID-5, The Personality Inventory for DSM-5; SGI, Sensory Gating Inventory. Perceived contrast difference (%) refers to the degree to which the reference grating contrast was reduced to match the perceived contrast of the target grating. Width (w) represents tuning width, with broader tuning width reflecting less rapid decay of suppression across relative orientations; Magnitude (M); parameter represents sensitivity to orientation: greater negative M suggest greater reductions in suppression as relative orientation approaches 90°. Offset (o) parameter estimating orientation-insensitive (untuned) suppression (evident even at 90°). w, M , ow_{N1}; estimated from exponential decay function fit to contrast perception (behavioral) data; $w_{N1,}$ M_{N1}, o_{N1}; same parameters derived using N1 data. Alpha for post hoc contrasts set to .05, and P-values were corrected for false discovery rate (FDR).

[a]Adjusting for influence of visual acuity removes this difference.

were located at 3° eccentricity, 16° of polar angle below the horizontal meridian so that stimuli would have a lateralized cortical representation. Stimuli were generated using PsychoPy (version 1.85.2).[44] The contrast of the target was kept constant at 80%, whereas the contrast of the reference was adjusted to achieve a match in perceived contrast. The side on which the reference/surround stimuli was presented was randomized, with stimuli appearing in the left and right visual fields with equal frequency and probability. The contrast of the reference grating was controlled by a separate Psi staircase[45] implemented in PsychoPy for each relative orientation. Each staircase converged at a point of subjective equality between the reference grating (for which contrast was varied) and target (fixed contrast) grating. Supplementary figure S1 depicts the stimulus presentation paradigm, as well as the surround condition stimuli used for the ODSS task.

The key behavioral index generated from the task was the degree to which the contrast of the reference (no surround) needed to be reduced to match the perceived contrast of the target grating with a surround (ie, perceived contrast difference %; see table 1). We characterized the relative dependence of each participant's suppression on orientation by applying an exponential decay function to contrast decrement data: $P = -Me^{-\theta/w} + o$. Model fitting was implemented using the *scipy.optimize.curve_fit* algorithm in Python. The offset parameter (o) approximates orientation-insensitive (ie, untuned) surround suppression with greater negative o reflecting enhanced suppression of target contrast irrespective of orientation. The magnitude (M), and tuning width (w) jointly characterize orientation-dependent (ie, tuned) surround suppression. Greater negative M reflects greater orientation selectivity, in contrast, surround suppression, or the degree to which suppression of target contrast is reduced as relative surround orientation approaches orthogonality. The w parameter reflects the width of orientation tuning: larger (more positive) values reflected broader width in orientation tuning. Supplementary figure S2 provides verbal description for the interpretation of these parameters, and visually depicts how changing the free parameter values influences the exponential decay function. Visualizations of group differences in the o, M, or w parameters, and the average fit for each diagnostic group are presented in supplementary figure S3.

EEG Collection and Surface Laplacian Transformation of VEP

EEG data were collected using a Brain Vision 128-channel actiChamp system at a sampling rate of 1000 Hz, with the average of the earlobe (mastoid) electrodes used as a reference for visualization. Trials were epoched from 500 ms prestimulus to 1000 ms poststimulus, and submitted to Independent Components Analysis using a custom pipeline (ICAcleanEEG[46]; see supplementary materials for additional details). Supplementary table S3 presents the number of ICs that were judged to be nonneural noise, and therefore excluded from further processing. After generating subject-average VEP, we applied the surface Laplacian transform using the Current Source Density toolbox[40] (spline density [m] = 3, smoothing constant [λ] = 1^{-5}). This transformation produces a current source density (measured in $\mu V/cm^2$) that emphasizes radially oriented superficial cortical sources at the exclusion of deep focal sources, or superficial but spatially diffuse cortical activity. Current source density estimates represent a spatial enhancement of neuronal activity at the scalp.[47]

Time windows for the P1 [50–140 ms] and N1 [120–225 ms] were defined by examining the distribution of participants' peak latencies via butterfly plots, and grand-averaged VEP that were collapsed across diagnostic group and stimulus conditions (ie, relative orientation of the surround) inspected via topographical distributions in EEGLAB.[48] We pooled current source density estimates for the P1 across 8 electrodes: PO8, PO10, P8, and P6 in right hemisphere to targets presented in left hemifield, and PO7, PO9, P7, and P5 in left hemisphere to targets presented in right hemifield (ie, contralateral P1; see figure 1A and supplementary figure S4). Contralateral N1 estimates were pooled across 10 electrodes: PO8, PO10h, O2, PO4, and PO6h in the right hemisphere and PO7, PO9h, O1, PO3, and PO5h in the left hemisphere (see figure 2A and supplementary figure S5). To examine group differences in N1 hemispheric asymmetry, we generated difference waves by subtracting left contralateral N1 from right contralateral N1 (see figure 3A). Choice of electrodes was based on where response was maximal to surrounds presented in right and left visual field in order to characterize hemifield-dependent neural activity in striate and extrastriate visual cortices, in accordance with prior work.[22,36,43,49] Peak latency of the P1 and N1 component did not vary as a function of relative surround orientation, or diagnostic group. Peak latency values are presented in supplementary table 1, with grand-average waveforms of the P1 and N1 presented in supplementary figures S4 and S5.

We then applied the exponential decay function used for behavioral analyses to participants' mean N1 response at each orientation to characterize neurophysiological aspects of tuned and untuned suppression.[18,19] The relevant parameters of interest included the offset (o_{N1}) approximating orientation-insensitive surround suppression evident in the N1, the magnitude (M_{N1}), and tuning width (w_{N1}), jointly characterized the neural correlates of tuned suppression evident in the N1. To facilitate direct comparisons between the behavioral and N1 parameters, we calculated the additive inverse (ie, reverse the sign by multiplying values by −1) of the o_{N1} and M_{N1} to align the direction of effects (see supplementary figure

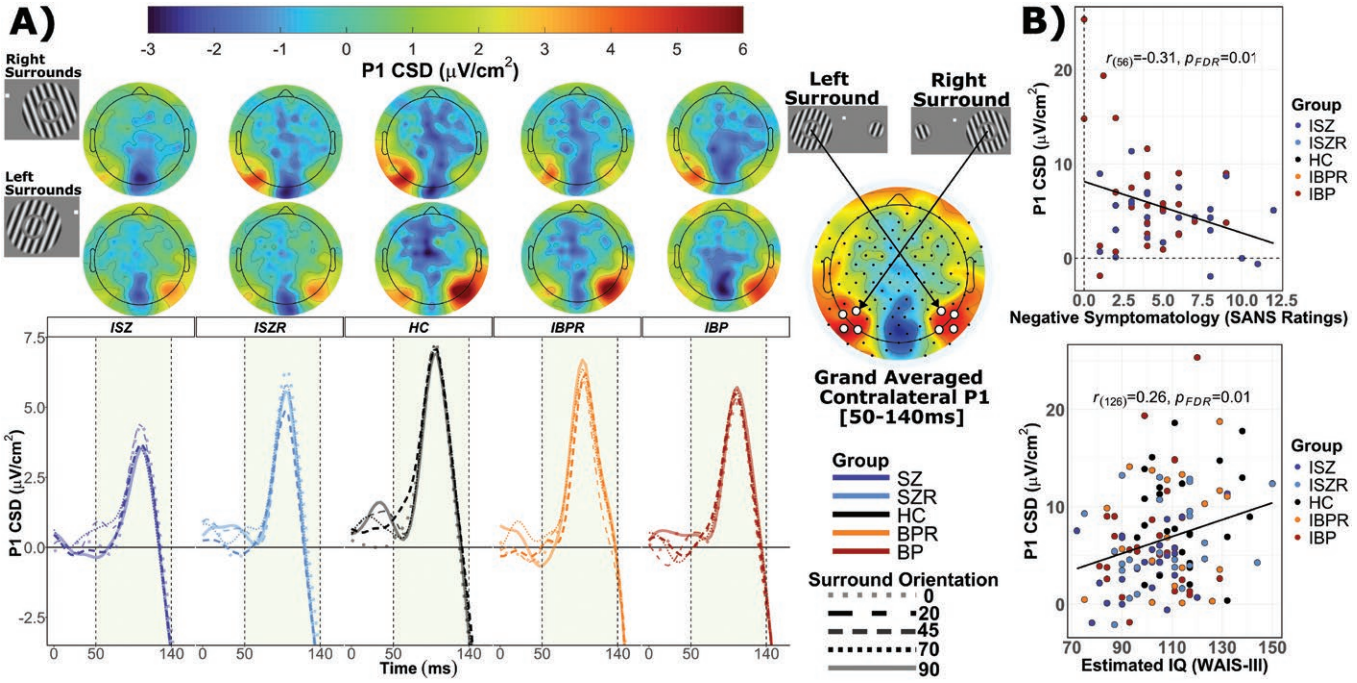

Fig. 1. Group differences in P1 waveforms. (A) Top panel depicts group-averaged P1 topographies to left and right surrounds (μV/cm^2). Group topographies are scaled to HC P1 response to left surrounds (ie, right contralateral P1, where response was maximal). The diagram on the right depicts grand-averaged (ie, averaged across all conditions and participants) P1 topographies. Electrodes highlighted in white represent the contralateral electrodes (ie, hemisphere opposite to visual hemifield where surround was presented) in the left and right hemispheres from which P1 was pooled. The bottom panel depicts group-averaged P1 to different surround orientations, which were averaged across hemispheres. P1 was reduced in ISZ relative to HC, ISZ, and ISZR ($P_{FDR} < .001$) and ISZR ($P_{FDR} < .05$), with ISZR and ISZR demonstrating intermediate reductions relative to HC ($P_{FDR} < .01$). (B) The top panel depicts the negative association between P1 CSD and negative psychotic symptomatology in probands ($r(126) = -0.31$, $P_{FDR} = .01$), while the bottom shows the positive association between P1 CSD and IQ across the full sample ($r(126) = 0.26$, $P_{FDR} = .01$).

S2), and to make interpretation of parameter values consistent. Supplementary figure S6 depicts group differences in these parameters, in addition to the average fit of the exponential decay function applied to participants' N1 response.

Statistical Plan

Group Comparisons and Partial Correlations. All statistical analyses were conducted using *R* (Version 4.2.2).[50] To examine group differences in the P1 and N1 component, we used generalized least squares regression to account for correlated-error structures (ie, repeated measures), and to model nonconstant error (ie, heteroscedasticity) between diagnostic groups.[51] These models were fit using the *gls* function in the *nlme* package,[52] and specified the following main effects: Diagnostic Group (5 levels: ISZ, ISZR, HC, IBPR, and IBP), Surround Orientation (5 levels: 0°, 20°, 45°, 70°, and 90°), and Hemisphere (2 levels: Right and Left) as fixed effects. Post hoc analyses were conducted using the *emmeans* package,[53] with *P*-values corrected for the false discovery rate (FDR, denoted as P_{FDR}).[54] We conducted sensitivity analyses covarying for age, gender, and visual acuity (*LogMAR* scale) to account for their potential confounding effects on estimates of group differences in P1 and N1 responses,[55–57] and test whether visual acuity affected group differences in the neurophysiological correlates of contrast ODSS.[18,19] These analyses are presented in supplementary table S2 Greater age was associated with attenuated P1 and N1 responses ($P < .01$). Sex effects were evident in the P1 ($P < .01$), with males exhibiting larger amplitudes than females

We then examined whether alterations in early-latency VEP reflect neural correlates of tuned and/or untuned suppression. Specifically, we examined associations between the P1, N1, and N1 (right > left) hemispheric asymmetry with the tuned (ie, *M* and *w* parameters) and untuned (ie, *o* parameter) suppression mechanisms.[18,19] Estimates of contralateral P1 and N1 were averaged across stimulus conditions, yielding 3 neural indices in total. Correlations were performed with all participants (ie, collapsed across diagnostic groups) to increase statistical power. We computed partial Pearson correlations to account for the confounding effects of age and visual acuity on bivariate correlations (via inversion of covariance matrices) using functions in the *psych* package.[58]

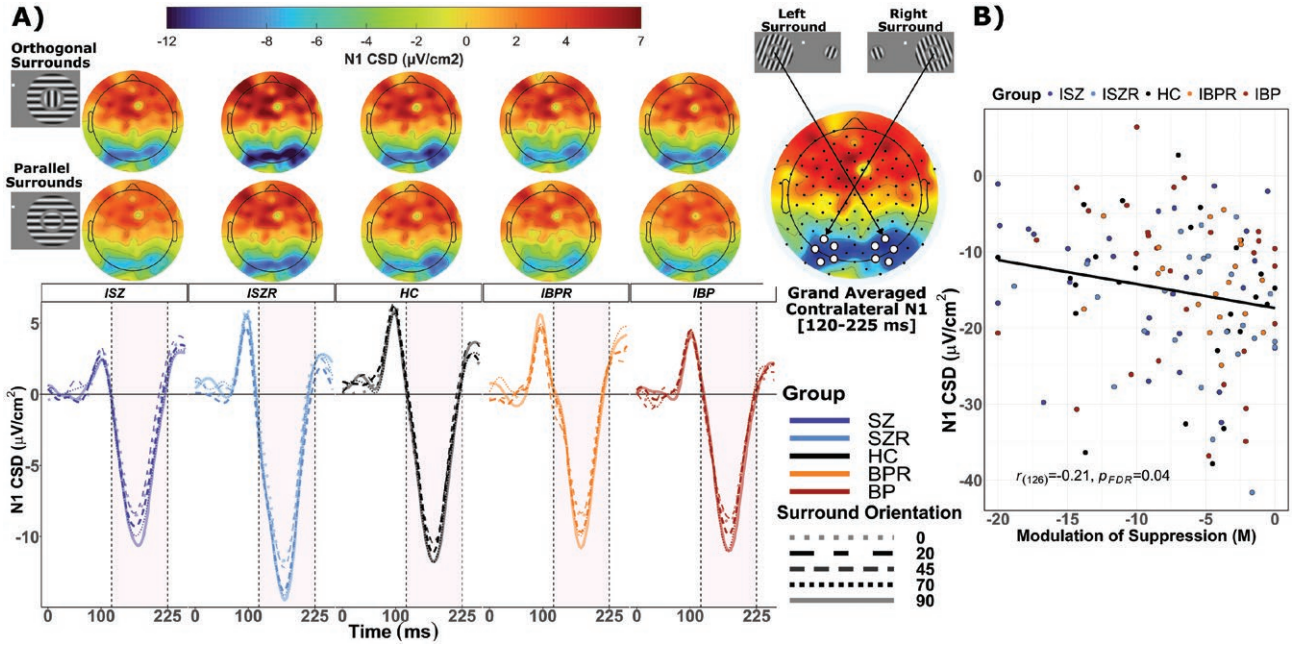

Fig. 2. Group differences in N1 waveforms. (A) Top panel depicts group-averaged N1 topographies to parallel and orthogonal surrounds ($\mu V/cm^2$) scaled to HC N1 response to orthogonal surrounds. The diagram on the right depicts grand-averaged (ie, averaged across all conditions and participants) N1 topographies. Electrodes highlighted in white represent the contralateral electrodes (ie, hemisphere opposite to visual hemifield where surround was presented) in left and right hemisphere where N1 was pooled. The bottom panel depicts group-averaged N1 to different surround orientations, which were averaged across hemispheres. N1 was reduced in ISZ, ISZ, and ISZR relative to HC ($P_{FDR} < .001$) and ISZR ($P_{FDR} < .05$). (B) The top scatterplot depicts the negative association between N1 and modulation of suppression, ie, the degree to which contrast suppression *decreases* as orientation increases from parallel to orthogonal ($r(126) = -0.21$, $P_{FDR} = .04$) where more negative values for *M* represent more orientation-dependent suppression.

Associations with the P1 index also accounted for sex effects. We adjusted all *P*-values for FDR to reduce type I error while maintaining statistical power.[52]

Research suggests that atypical surround suppression is greatest in more symptomatic individuals,[10,59] and may reflect a continuum of severity related to genetic and dimensional aspects of psychotic psychopathology.[13,18,19] Accordingly, we examined associations between these neural indices and measures that relate to genetic liability for psychosis[37,60]: (1) a dimensional measure of psychotic psychopathology (ie, trait psychoticism from the Personality Inventory for DSM-V)[61]; and (2) real-world anomalous perception (ie, the Sensory Gating Inventory[62]). Alterations in visual P1 are thought to reflect a trait marker of psychosis, which may relate to atypical gain control in individuals with psychotic psychopathology.[63,64] Thus, we examined associations between the neural indices and: (1) global cognitive function (ie, estimated global cognition from the Wechsler Adult Intelligence Scale-III); and (2) and negative psychotic symptomatology (ie, global negative symptom the Scale for the Assessment of Negative Symptoms) to examine whether disrupted low-level visual functioning is associated with measures linked to functional outcomes and illness severity.[65–67] Collectively, these exploratory analyses sought to leverage our transdiagnostic sample to test whether alterations in neurophysiology during contrast perception are associated with the expression of symptom domains that cut across psychiatric disorders, and linked to phenotypic expression along the psychosis continuum.[68,69]

We conducted sensitivity analyses using linear-mixed effects models with a random group intercept for the diagnostic group to ensure these associations were not inflated by mean differences between groups.[70,71] Critically, the associations remained significant. Details can be found in supplementary methods, with modeling results presented in supplementary table S3. Finally, we examined the associations between the parameters of the exponential function for behavioral (*M, o,* and *w*) with those of the N1 VEP (ie, M_{N1},o_{N1}, and w_{N1}). Supplemental analyses exploring linkages between participants' mean N1 response and contrast suppression at each surround orientation are presented in supplementary figures S4 and S5.

Group Comparisons in Nonlinear Associations: Generalized Additive Mixture Models. We applied Generalized Additive Models (GAMMs) to further evaluate the effect of ODSS on contrast perception and N1 responses across all target-surround relative orientations. GAMMs are semi-parametric, integrating fixed effect estimates via both parametric (ie, predictor follows predetermined form) and nonparametric functions (ie, predictor is quantitatively derived using algorithmic approaches), classified as "smooths." As a result, they are

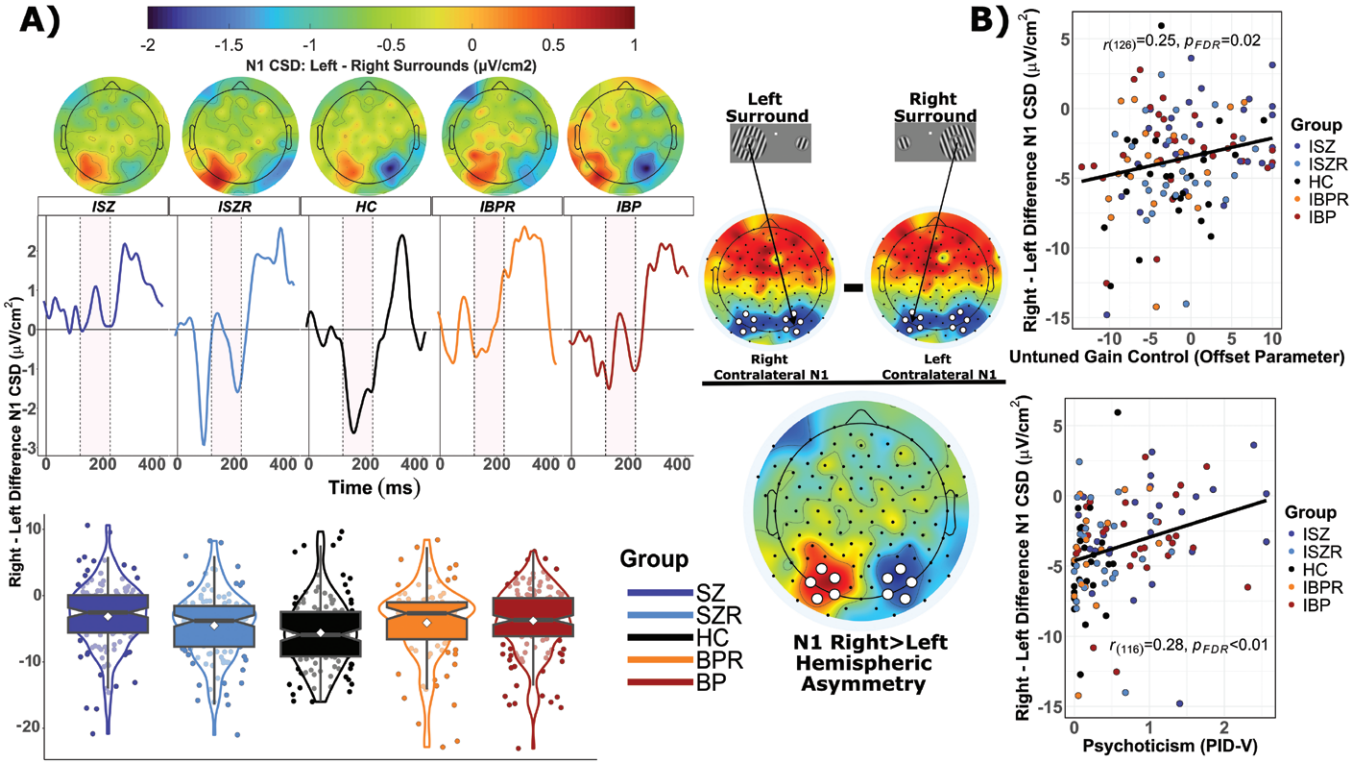

Fig. 3. Group differences in N1 right > left hemispheric asymmetry. (A) The topographies depict the group-averaged N1 difference to left surrounds—right surrounds (μV/cm^2), scaled to HC difference to left-right surrounds (ie, where N1 asymmetry was maximal). The waveforms below the topographies depict the right > left hemispheric asymmetry in N1 averaged across conditions and hemispheres. The diagram on the right depicts how the asymmetry was calculated. Electrodes highlighted in white represent the contralateral electrodes (ie, hemisphere opposite to visual hemifield where surround was presented) where N1 was pooled. The boxplots depict group differences in the N1 hemispheric asymmetry across conditions, with the white diamonds representing group median values, and the center line representing group mean values. The degree of right > left asymmetry in the N1 was reduced in ISZ relative to HC ($P_{FDR} < .05$). (B) The top scatterplot depicts the association between the degree of right > left N1 hemispheric asymmetry and psychoticism. Greater trait psychoticism was associated with reduced right > left hemispheric asymmetry in the N1 ($r(116) = 0.28$, $P_{FDR} < .01$). The bottom scatterplot depicts the association between the degree of N1 asymmetry and untuned suppression. Weakened untuned suppression (ie, more positive *o* parameter values) was associated with reduced hemispheric asymmetry in N1 ($r(126) = 0.25$, $P_{FDR} = .02$). In other words, a reduction in the overall influence of the surround on the perceived contrast of the central stimulus, which we previously demonstrated was diminished in ISZ[18] was associated with reduced right > left hemispheric asymmetry in the N1 that was uniquely absent in ISZ.

well-suited to approximate the additive and interactive effects of linear and nonlinear phenomena underlying visual functions such as contrast sensitivity and gain control.[72,73] Accordingly, we leveraged these properties to test whether ISZ exhibit alteration in nonlinear functions characterizing ODSS. GAMMs were fit using the *mgcv* package using Restricted Maximum Likelihood to optimize estimation of the smoothing parameter (λ).[74] We implemented an extension of the traditional GAMM framework, wherein the associations between predictor and outcome variables vary across group levels (ie, exhibit a hierarchical structure).[75]

Models were first fit with a parametric effect of diagnostic group, as well as a nonparametric "global" (ie, main effect) smooth for relative surround orientation that characterized the nonlinearity in orientation selectivity in contrast and N1 suppression across subjects (figure 4A and B).[75,76] We also included a "factor-smooth" interaction term that specified a distinct smoothing function between the outcome variable and relative orientation for each diagnostic group (figure 4C and D). Post hoc tests are performed by specifying the coding of model contrasts as treatment contrast,[77] with HC serving as the "control group" or reference level. This yields $R - L$ "difference smooths," where $l = R, \ldots, L$ are the levels of a factor, R is the reference group, and L is the number of levels. These "difference smooths" correspond to the overall difference between the smooth function estimated for the reference level R, and the smooth function estimated for the lth level of a factor. A significant result suggests that the lth level of the factor, or "treatment group" (ISZ, ISZR, IBPR, and IBP), exhibits a different relationship between ODSS, and/or N1 response, as a function of relative orientation compared to the reference level, or "control group" (HC).[75,78,79] Importantly, this only suggests an atypical relationship in ODSS, and limits more nuanced conclusions about tuned suppression mechanisms. A significant parametric effect suggests the difference in mean

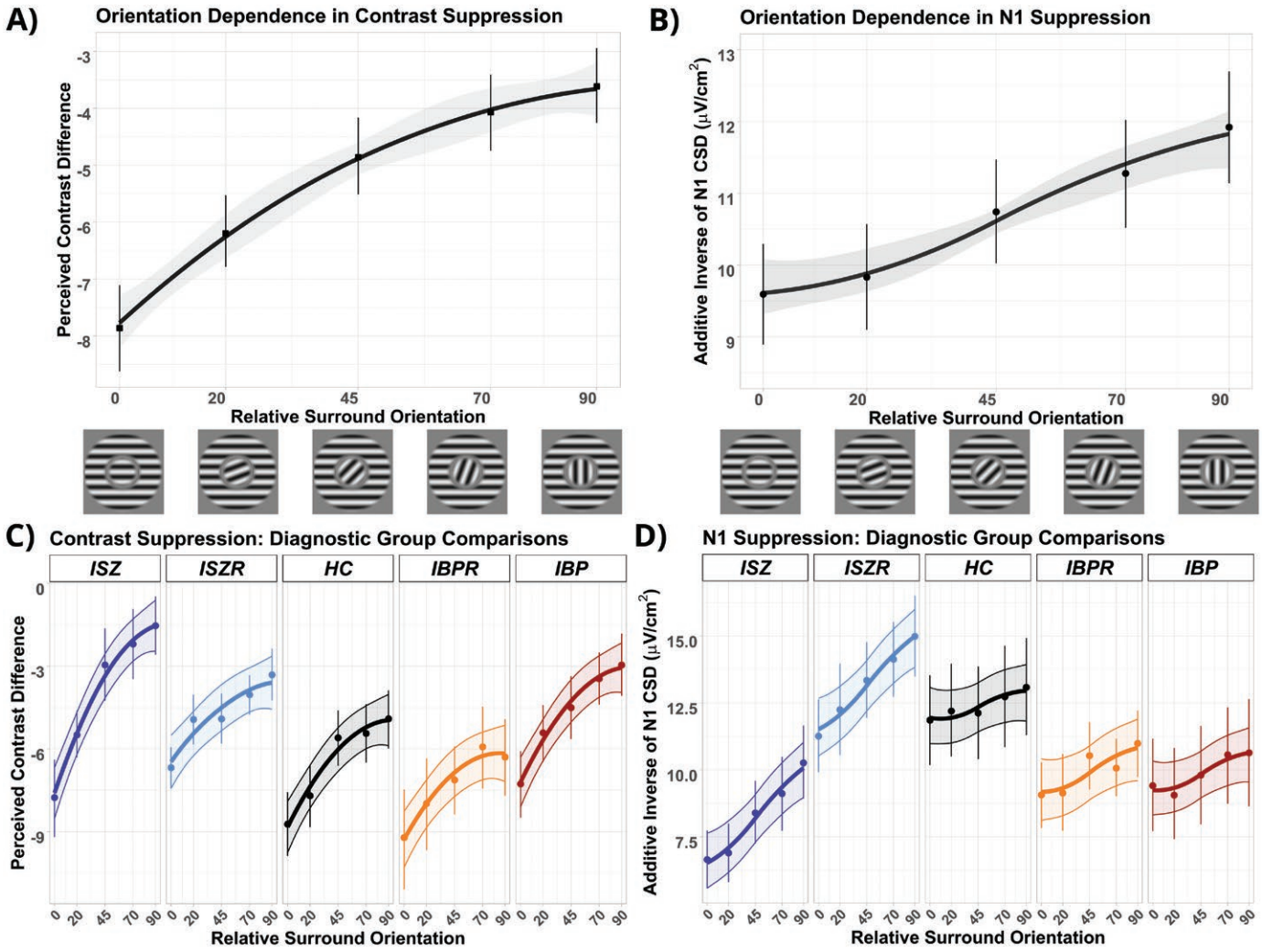

Fig. 4. Orientation sensitivity evident in contrast suppression and N1 response using generalized additive mixture models (GAMMs). (A) The black line depicts the "global" (main effect) of orientation collapsed across participants for contrast suppression, which was strongly nonlinear (*edf* = 3.82, $P < .001$). The band around the black line depicts the 95% CI of model estimates. (B) The black line depicts the "global" (main effect) of orientation collapsed across participants on the N1 response, which was strongly nonlinear (*edf* = 2.99, $P < .001$). The band around the black line depicts the 95% CI of model estimates. (C) Visual depiction of the "factor-smooth" interaction, which examines the nonlinear relationship between contrast suppression and orientation. Lines depict the nonlinear associations of perceived contrast difference as a function of orientation for each diagnostic group, while the band around lines depicts ± the standard error of model estimates. SZ (*edf* = 3.31, $P_{FDR} < .01$) exhibited more rapid decreases in suppression with increasing orientation relative to HC (*edf* = 2.72). (D) Visual depiction of the "factor-smooth" interaction, which examines the nonlinear relationship between N1 response and orientation. Lines depict the nonlinear associations of the N1 response as a function of orientation for each diagnostic group, while the band around lines depicts ±1 standard error of model estimates. Both ISZ (*edf* = 2.85, $P_{FDR} < .01$) and ISZR (*edf* = 2.43, $P_{FDR} < .01$) exhibited greater decreases in N1 suppression relative to HC (*edf* = 1.35).

values between HC and the *l*th level of a factor significantly differs from 0. Because parametric effects can only operate to shift a function up or down along the *y*-axis, they represent group intercepts at each orientation. The interpretation of the statistical effect is akin to the offset parameter (*o*), because it implies a consistent difference across orientations, or a greater overall influence of the surround.

We specified 2 GAMM models examining group differences in contrast perception, and N1 response. Nonindependence of observations was accounted for by including a random-intercept for each participants' contrast suppression or N1 response data at each orientation. We applied the double shrinkage penalty (a robust method of variable selection) to perform model selection. Critically, this also narrows the credible confidence interval of the parametric and nonparametric effects estimated by GAMMs to enhance confidence the results of statistical tests and corresponding confidence and simultaneous intervals of factor-smooth terms.[78,80,81] We used functions in the *gratia, itsadug,* and *mgcv* packages to perform model diagnostics, and

extract model predictions and derivatives.[78,82] These analyses allowed us to test whether ISZ is associated with atypical nonlinear associations in the degree of surround suppression in contrast perception as function of relative orientation, and whether these atypical associations are evident in the neural correlates of ODSS (ie, N1 response). As with the exponential decay function, we transformed participants' N1 responses by calculating the additive inverse to facilitate ease of comparison of GAMM results for both contrast and N1 suppression (see figure 4A and B).

Results

Behavioral Results: Group Comparisons Accounting for Visual Acuity

Group comparisons of task performance and ODSS mechanisms estimated from the exponential decay function parameters are presented in table 1 and visualized in supplementary figure S3. A regression model estimating group differences in the *o* (offset) parameter revealed an effect of diagnostic group ($F_{4,123} = 4.22$, $P < .01$), but not of acuity ($F_{1,123} = 0.04$, $P = .84$). Post hoc tests revealed ISZ had more positive *o* values compared to BPR and HC ($P_{FDR} < .05$). Similarly, a regression model estimating group differences in the *M* parameter revealed an effect of diagnostic group ($F_{4,123} = 3.30$, $P = .01$) and visual acuity ($F_{1,115} = 16.88$, $P < .001$), with worse acuity relating to greater orientation-sensitive suppression. Post hoc tests did not survive correction for FDR. Analyses excluding visual acuity revealed ISZ to have larger negative values of *M* relative to HC. There were no effects of group ($F_{4,123} = 0.63$, $P = .64$), or acuity ($F_{1,123} = 0.98$, $P = .32$) on the *w* parameter, which characterizes the tuning width of orientation-sensitive mechanisms.

Contralateral P1 VEP: Parametric Effects

Group-averaged P1 waveforms at electrode sites contralateral to the visual field with the surround (denoted with white circles) are presented in figure 1A. There were effects of group ($F_{4,125} = 8.1$, $P < .001$), and hemisphere ($F_{1,125} = 21.9$, $P < .001$), reflecting a larger P1 in right than left hemisphere, but no effect of relative surround orientation; ($F_{4,125} = 0.19$, $P = .94$). Post hoc analyses of the main effect of group indicated that ISZ (mean [*M*] = 3.2 μV/cm^2, standard error [*SE*] = 0.28) had the greatest reductions in P1 relative to HC ($M = 6.1$ μV/cm^2, $SE = 0.31$; $P_{FDR} < .001$, $d = -0.69$). ISZ P1 was also reduced relative to IBP ($M = 4.7$ μV/cm^2, $SE = 0.32$; $P_{FDR} < .01$, $d = -0.37$) and IBPR ($M = 5.3$ μV/cm^2, $SE = 0.42$; $P_{FDR} < .01$, $d = -0.50$). Differences between ISZ and ISZR ($M = 4.1$ μV/cm^2, $SE = 0.32$; $P_{FDR} = .04$, $d = -0.23$) were less pronounced. ISZR ($d = -0.46$, $P_{FDR} < .01$) and IBP ($d = -0.32$, $P_{FDR} < .01$) exhibited reduced P1 relative to HC, while IBPR exhibited larger responses compared to ISZR ($P_{FDR} = .04$, $d = 0.28$).

Partial correlations accounting for age, biological sex, and visual acuity revealed that P1 averaged across stimulus conditions was negatively related to SANS global ratings in probands ($r(56) = -0.32$, $P_{FDR} = .03$), such that reduced P1 was associated with a greater degree of negative psychotic symptomatology (figure 1B [top]). There was also a positive association between P1 and IQ ($r(126) = 0.25$, $P_{FDR} = .01$; figure 1B [bottom]) suggesting that reduced P1 during stimulus viewing was related to worse cognitive functioning.

Contralateral N1 VEP: Parametric Effects

Group-averaged N1 waveforms at electrode sites contralateral to the visual field with the surround (denoted with white circles) are presented in figure 2A. There were effects of group ($F_{4,125} = 3.9$, $P < .001$), and relative surround orientation ($F_{4,125} = 6.3$, $P \leq .01$), but not hemisphere ($F_{1,125} = 1.2$, $P = .27$) on the N1. Regarding the effects of relative orientation: N1 was reduced at 0° relative surround orientation ($M = -10.0$ μV/cm^2, $SE = 0.40$), compared to 70 ($M = -11.6$ μV/cm^2, $SE = 0.41$; $P_{FDR} = .02$, $d = 0.20$) and 90° ($M = -11.9$ μV/cm^2, $SE = 0.40$, $P_{FDR} < .01$, $d = 0.24$). N1 was also reduced at 20° ($M = -10.2$ μV/cm^2, $SE = 0.41$) compared to 90° ($P_{FDR} = .02$, $d = 0.21$). Considering the effects of Group: post hoc analyses indicated that ISZ ($M = -9.02$ μV/cm^2, $SE = 0.52$, $d = -0.51$), and IBP ($M = -9.92$ μV/cm^2, $SE = 0.60$, $d = -0.38$) had reduced N1 relative to HC ($M = -12.72$ μV/cm^2, $SE = 0.59$; all $P_{FDR} < .05$). ISZR ($M = -13.63$ μV/cm^2, $SE = 0.52$) had larger N1 compared to ISZ ($d = 0.64$), IBP ($d = 0.51$), and IBPR ($M = -10.4$ μV/cm^2, $SE = 0.51$, $d = 0.42$). Partial correlations accounting for age and visual acuity demonstrated that N1 averaged across stimulus conditions was negatively related to the *M* parameter ($r(126) = -0.27$, $P_{FDR} < .01$) such that smaller N1 amplitudes were associated with greater release from suppression as relative orientation of center and surround progressed from parallel to orthogonal.

N1 Hemispheric Asymmetry: Parametric Effects

Evidence suggests that ISZ is associated with a reduced rightward asymmetry that may reflect difficulties maintaining attention across visual hemifields and may be evident in N1 response.[41,43,83] Accordingly, we examined group differences in this rightward asymmetry by subtracting the N1 response to right surrounds from the N1 response to left surrounds. There was an effect of group ($F = 2.91$, $P = .02$), but not relative surround orientation ($F = 0.86$, $P = .46$) on the degree of hemispheric asymmetry (right > left) for N1. Follow-up pairwise comparisons revealed that ISZ ($M = -1.5$ μV/cm^2, $SE = 0.51$) had reduced N1 asymmetry compared to HC ($M = -3.2$

μV/cm², $SE = 0.52$; $P_{FDR} = .02$, $d = 0.56$). Topographies depicting (right > left) N1 hemispheric asymmetry are presented in figure 3A.

Partial correlations accounting for participants' age and visual acuity indicated that the degree of asymmetry toward the right hemisphere in the N1 was associated with greater atypical perceptual modulation as reported on the Sensory Gating Inventory ($r(120) = 0.24$, $P_{FDR} = .03$). Reduced rightward asymmetry in the N1 was also associated with greater self-reported psychoticism on the Personality Inventory for the DSM-V ($r(116) = 0.24$, $P_{FDR} = .04$; figure 3B [top]). Finally, the asymmetry of the N1 was associated with larger *o* parameter values from the model of behavior ($r(126) = 0.25$, $P_{FDR} = .01$; figure 3B [bottom]), weakened untuned suppression (ie, more positive *o* parameter values) was associated with reduced hemispheric asymmetry in N1.

Tuned and Untuned Suppression in the N1 VEP

Table 1 displays group-level means and standard deviation for parameters of exponential decay function applied to participants' N1 response. A visualization of group differences of these parameters is depicted in supplementary figure S6. There were no effects of diagnostic group on the w_{N1} ($F_{4,125} = 0.58$, $P = .67$), or o_{N1} ($F_{4,125} = 1.37$, $P = .21$). In contrast, there was an effect of diagnostic group on the M_{N1} parameter ($F_{4,125} = 2.86$, $P = .03$) with ISZ exhibiting stronger (more negative) M_{N1} relative to HC ($P_{FDR} = .03$).

Models of Nonparametric Effects in Behavioral Data: GAMMs

The application of GAMMs allows for a parametric but model-free characterization of behavioral measures of contrast perception. Consistent with previous analyses, there was an effect of diagnostic group ($F_{4,123} = 4.35$, $P < .01$) with ISZ ($t = 3.02$, $P_{FDR} < .01$) and IBP ($t = 2.22$, $P_{FDR} = .03$) having reduced contrast decrement relative to HC across surround orientations. Nonparametric effects of the GAMMs analysis included a main effect of visual acuity (*edf* = 1.0, $F_{1,123} = 6.13$, $P < .01$), with worse acuity predicting greater suppression across surround orientations. There was a strong nonlinear effect of orientation (*edf* = 3.82, $F_{1,123} = 62.12$, $P < .001$; figure 4A), indicative of contrast suppression being modulated by the relative orientation of the surround. There was also an interaction between diagnostic group and surround orientation ($F_{8,123} = 3.12$, $P < .001$), indicating that as the relative orientation of the surround varied, diagnostic groups differed in the degree of contrast suppression of the target (figure 4C). ISZ (*edf* = 3.31, $F = 5.36$ $P_{FDR} < .01$) exhibited greater decreases in contrast suppression with increased orientation mismatch (ie, greater release from suppression) suggesting ISZ exhibited greater orientation sensitivity in contrast suppression relative to HC (*edf* = 2.72).

Models of Nonparametric Effects in N1: GAMMs

Through the application of GAMMs we also characterized parametric effects on the N1 VEP during ODSS. Consistent with the linear analysis there was an effect of diagnostic group ($F_{4,125} = 4.35$, $P < .01$) with ISZ ($t = 2.52$, $P_{FDR} = .04$) having reduced N1 relative to HC across relative surround orientations. Nonparametric effects of the model included a main effect of orientation indicating that the N1 was modulated by surround orientation and that the relationship was highly nonlinear (*edf* = 2.99, $F_{1,125} = 11.36$, $P < .001$; figure 4B). There was no effect of visual acuity on the N1 (*edf* = 1.0, $F_{1,125} = 0.01$, $P = .97$). There was also an interaction of group and orientation ($F_{8,125} = 3.59$, $P < .01$) indicating that as the relative orientation of the surround varied, diagnostic groups differed in their N1 amplitudes (figure 4D). ISZ (*edf* = 2.85, $F = 5.36$, $P_{FDR} < .01$) and ISZR (*edf* = 2.43, $F = 5.42$, $P_{FDR} < .01$) exhibited greater decreases in N1 suppression relative to HC (*edf* = 1.35) as the relative orientation between center-surround became closer to orthogonal (ie, greater orientation sensitivity).

Discussion

We sought to better understand atypical surround suppression in individuals with psychotic psychopathology (ie, ISZ and IBP)[19] and their first-degree relatives (ie, IBPR and ISZR)[18] by examining whether early visual neural functions (ie, N1 and P1) correlated with alterations in the perceived contrast of a center stimulus that depended on the characteristics of a surrounding stimulus. Both ISZ and ISZR showed evidence that the perceived contrast of the center was more dependent than HCs on the alignment of grating patterns within the center and surround stimuli. The increased dependency of perceived contrast on the relative orientation of center and surround gratings indicates an *enhanced* influence of tuned suppression (ie, dependent on relative orientation of gratings) in psychotic psychopathology. The dependency of suppression on relative orientation was mirrored in the early visual response over the occipital hemisphere contralateral to the visual field of the surround: ISZ and ISZR exhibited a suppression of N1 amplitudes that was more strongly dependent than HCs on alignment of grating patterns within the center and surround (figure 4D). Interestingly, ISZ also exhibited a smaller asymmetry of N1 amplitudes toward the right occipital hemisphere which was associated with greater psychotic psychopathology and *reduced* untuned suppression (measured as the amount of perceptual suppression by orthogonal surrounds). Neither indicator of enhanced tuned nor reduced untuned contrast suppression were related to bipolar disorder, although

both ISZ and IBP showed overall reductions in N1 amplitudes. Results indicate that atypical contextual effects on visual perception in schizophrenia derive from both orientation-sensitive and insensitive mechanisms, while genetic liability for schizophrenia is associated with an enhanced sensitivity to orientation during surround suppression.

Disruptions in the neural correlates of ODSS are evident along a continuum of psychotic psychopathology and are consistent with our previous characterizations of atypical untuned suppression mechanisms.[18,19] Collectively, these alterations in contrast suppression and neurophysiological responses appear related to anomalous visual functioning[59] and contribute to atypical visual perceptual phenomena in psychosis,[84] given the associations we found with real-world anomalous perception and psychotic psychopathology. Thus, results of the present study point to specific early neurophysiological responses that may account for the altered use of visual context in psychotic psychopathology. Notably, findings of increased, rather than decreased, effects of orientation sensitivity rule-out some nonspecific effects, such as poor fixation and increased error rates, driving these effects.[11,85]

Unlike the N1 component, which was sensitive to both tuned and untuned aspects of surround suppression, the earlier P1 component contralateral to the visual field of the surround was insensitive to the effects of the surround on perceived contrast of the center stimulus. Nevertheless, P1 amplitude was reduced in ISZ, and modestly reduced in IBP and ISZR. Reduced P1 was associated with greater negative psychotic symptomatology and lower intelligence. P1 reductions exhibited by ISZ replicates a consistent neurophysiological finding in the disorder evident during low-level (eg, contrast sensitivity)[35,86] and higher-level (eg, perceptual closure)[87,88] visual functions. This suggests reduced P1 may reflect alterations in early visual cortical responses underlying atypical visual perception in psychosis, perhaps as a result of alterations in visual gain control in extrastriate cortices.[34,89] Modest reductions of P1 in ISZR and IBP are consistent with studies involving other visual paradigms that documented reduced P1 in first-degree relatives,[90] and IBP.[91] Therefore, attenuated P1 may reflect a transdiagnostic anomaly related to genetic and dimensional aspects of psychotic psychopathology, wherein disruptions in early-latency VEP reflect atypical visual gain control that is greatest in individuals with a psychotic disorder.[18,19,92–94] Results of the present work provide evidence that atypical gain control is related to cognitive difficulties and negative symptomatology, which are associated with worse functional outcomes in individuals with psychotic psychopathology.[65,95]

Suppression of N1 response to target stimuli was greatest at parallel surrounds and weakest to orthogonal surrounds, consistent with ODSS (figure 2A).[13,15] The N1 was additionally associated with greater orientation sensitivity during suppression of perceived target contrast as measured by the *M* parameter of the ODSS model (figure 2B). Concurrently, attenuated N1 responses were associated with greater orientation sensitivity (larger negative *M*), perhaps reflecting greater contrast suppression as gratings of the target, and surround became parallel. GAMM results suggest the orientation selectivity of N1 responses conform to a nonlinear decay in suppression with increasing relative orientation (figure 4A and B). Tuned suppression mechanisms during contrast perception have been characterized in psychophysical studies and related to primate neurophysiology.[2,14–16,25,96] Hence, experimental results are aligned with prior work demonstrating that the N1 reflects a neural correlate of ODSS during contrast perception,[22] and suggest that the generation of early visual response reflects the influence of tuned suppression mechanism.[14,22,32,97] Tuned suppression is determined by either alterations in feedback activity to V1 from higher-level visual areas (eg, V4 or lateral occipital cortex)[13,14,32] or V1-intrinsic mechanisms (ie, horizontal propagation of lateral connections in V1). It is also important to note that individuals affected by severe psychopathology (ISZ and IBP) exhibited attenuated N1 responses overall. In contrast, ISZR exhibited larger N1 which may reflect compensatory neural responses during visual discrimination of the task.[98–100]

Our investigation also revealed a rightward hemispheric asymmetry in the N1 as participants completed the ODSS task (figure 3A). This lateralization may reflect the specialization of the right hemisphere in visuospatial attention to process features across the target center, surround, and reference.[41,42,83,96,101–103] The distinct lack of asymmetry in ISZ may relate to disrupted functions of the right cerebral hemisphere which some researchers have posited in schizophrenia.[104–106] Indeed, participants with reduced lateralization in N1 response reported a greater degree of trait psychoticism and anomalous real-world perception, consistent with atypical lateralization reflecting a trait marker of schizotypy, and a neural mechanism associated with the psychosis continuum.[107–109] Reduced asymmetry of the N1 may reflect difficulties distributing attention across visual hemifields[83,110–112]; difficulties allocating spatial attention may account for the weakened untuned suppression exhibited by ISZ.[18]

Limitations

Methodological limitations preclude direct mechanistic linkages between neurophysiological results and surround suppression mechanisms. Orientation selectivity in the N1 responses could result from a feedback mechanism that mediates orientation sensitivity,[113] or a V1-intrinsic mechanism.[114–116] Also, future work should examine the role of neural oscillatory dynamics in atypical suppression mechanisms given their fundamental role in visual perceptual processes that are disrupted in psychosis.[117–122] Alpha oscillations are implicated as a V1-intrinsic

suppression mechanism, while gamma-synchronization is integral to receptive field dynamics underlying the processing surrounds[123,124]; both are implicated in GABAergic neurotransmission. Collectively, examining the role of neural oscillations may help clarify the neurophysiological mechanisms of ODSS, and test whether specific neural mechanisms in the visual system relate to more diffuse neural phenomena related to pathophysiological processes in psychosis.[125,126]

Conclusion

The present work examined whether alterations in early-latency visual neural functions were related to disruptions in visual suppressive mechanisms in ISZ.[18,19] We found evidence for disruptions of both untuned suppressive mechanisms (a reduction) and tuned suppressive mechanisms (greater dependence on relative orientation). These findings add to the growing evidence that ISZ experience alterations of function at many levels of the visual system.[98,127,128] Collectively, our findings highlight the utility of employing surround suppression paradigms to investigate atypical psychophysical and neurophysiological functions that span conventional diagnoses, and are related to genetic and dimensional aspects of psychotic psychopathology.[18,19,34]

Supplementary Material

Supplementary material is available at https://academic.oup.com/schizophreniabulletin/.

Acknowledgments

The authors would like to acknowledge funding from VA Merit Grant I01CX000227; NIH R01MH112583 and NIH U01MH108150. S.D.K. was supported by the National Institute of Drug Abuse T32DA050560. We are also deeply grateful to Andrea N. Grant for assistance with developing stimulus presentation code and for the hard work of the research assistants who helped collect data: Joseph Lupo, Haven Hafar, Abraham Van Voorhis, and Collin Teich. The authors have declared that there are no conflicts of interest in relation to the subject of this study.

Author Contributions

Conceptualization: C.A.O. and S.R.S. Methodology, C.A.O., S.R.S, Data Processing: S.D.K., C.T., V.J.P.; Formal analysis: S.D.K. Writing—Original: S.D.K. Writing—Review & Editing: C.A.O., S.R.S, C.T., E.R., and V.J.P; Visualization: S.D.K. Supervision of participant enrollment and assessment: S.R.S. Project Administration and Funding Acquisition: S.R.S.

References

1. Cavanaugh JR, Bair W, Movshon JA. Selectivity and spatial distribution of signals from the receptive field surround in macaque V1 neurons. *J Neurophysiol.* 2002;88(5):2547–2556. doi:10.1152/jn.00693.2001
2. Xing J, Heeger DJ. Measurement and modeling of center-surround suppression and enhancement. *Vis Res.* 2001;41(5):571–583. doi:10.1016/S0042-6989(00)00270-4
3. Supèr H, Romeo A, Keil M. Feed-forward segmentation of figure-ground and assignment of border-ownership. *PLoS One.* 2010;5(5):e10705. doi:10.1371/journal.pone.0010705
4. Hess R, Field D, Hess R, et al. Integration of contours: new insights. *Trends Cogn Sci.* 1999;3(12):480–486. doi:10.1016/S1364-6613(99)01410-2
5. Lamme VA. The neurophysiology of figure-ground segregation in primary visual cortex. *J Neurosci.* 1995;15(2):1605–1615. doi:10.1523/JNEUROSCI.15-02-01605.1995
6. Nothdurft HC, Gallant JL, van Essen DC. Response profiles to texture border patterns in area V1. *Vis Neurosci.* 2000;17(3):421–436. doi:10.1017/S0952523800173092
7. Phillips WA, Clark A, Silverstein SM. On the functions, mechanisms, and malfunctions of intracortical contextual modulation. *Neurosci Biobehav Rev.* 2015;52:1–20. doi:10.1016/j.neubiorev.2015.02.010
8. Silverstein SM, Lai A. The phenomenology and neurobiology of visual distortions and hallucinations in schizophrenia: an update. *Front Psychiatry.* 2021;12:684720. doi:10.3389/fpsyt.2021.684720
9. Barch DM, Carter CS, Dakin SC, et al. The clinical translation of a measure of gain control: the contrast-contrast effect task. *Schizophr Bull.* 2012;38(1):135–143. doi:10.1093/schbul/sbr154
10. Dakin S, Carlin P, Hemsley D. Weak suppression of visual context in chronic schizophrenia. *Curr Biol.* 2005;15(20):R822–R824. doi:10.1016/j.cub.2005.10.015
11. Tibber M, Anderson E, Bobin T, et al. Visual surround suppression in schizophrenia. *Front Psychol.* 2013;4:88. doi:10.3389/fpsyg.2013.00088
12. Knierim JJ, van Essen DC. Neuronal responses to static texture patterns in area V1 of the alert macaque monkey. *J Neurophysiol.* 1992;67(4):961–980. doi:10.1152/jn.1992.67.4.961
13. Shushruth S, Mangapathy P, Ichida JM, Bressloff PC, Schwabe L, Angelucci A. Strong recurrent networks compute the orientation tuning of surround modulation in the primate primary visual cortex. *J Neurosci.* 2012;32(1):308–321. doi:10.1523/JNEUROSCI.3789-11.2012
14. Nurminen L, Angelucci A. Multiple components of surround modulation in primary visual cortex: multiple neural circuits with multiple functions? *Vis Res.* 2014;104:47–56. doi:10.1016/j.visres.2014.08.018
15. Shushruth S, Nurminen L, Bijanzadeh M, Ichida JM, Vanni S, Angelucci A. Different orientation tuning of near- and far-surround suppression in macaque primary visual cortex mirrors their tuning in human perception. *J Neurosci.* 2013;33(1):106–119. doi:10.1523/JNEUROSCI.2518-12.2013
16. Trott AR, Born RT. Input-gain control produces feature-specific surround suppression. *J Neurosci.*. 2015;35(12):4973–4982. doi:10.1523/JNEUROSCI.4000-14.2015
17. Coen-Cagli R, Kohn A, Schwartz O. Flexible gating of contextual influences in natural vision. *Nat Neurosci.* 2015;18(11):1648–1655. doi:10.1038/nn.4128

18. Pokorny VJ, Schallmo MP, Sponheim SR, Olman CA. Weakened untuned gain control is associated with schizophrenia while atypical orientation-tuned suppression depends on visual acuity. *J Vis.* 2023;23(2):2. doi:10.1167/jov.23.2.2
19. Schallmo MP, Sponheim SR, Olman CA. Reduced contextual effects on visual contrast perception in schizophrenia and bipolar affective disorder. *Psychol Med.* 2015;45(16):3527–3537. doi:10.1017/S0033291715001439
20. Pedale T, Mastroberardino S, Capurso M, Macrì S, Santangelo V. Developmental differences in the impact of perceptual salience on short-term memory performance and meta-memory skills. *Sci Rep.* 2022;12(1):8185. doi:10.1038/s41598-022-11624-8
21. Keller AJ, Dipoppa M, Roth MM, et al. A disinhibitory circuit for contextual modulation in primary visual cortex. *Neuron.* 2020;108(6):1181–1193.e8. doi:10.1016/j.neuron.2020.11.013
22. Schallmo MP, Kale AM, Murray SO. The time course of different surround suppression mechanisms. *J Vis.* 2019;19(4):12–12. doi:10.1167/19.4.12
23. Bair W, Cavanaugh JR, Movshon JA. Time course and time-distance relationships for surround suppression in macaque V1 Neurons. *J Neurosci.* 2003;23(20):7690–7701. doi:10.1523/JNEUROSCI.23-20-07690.2003
24. Ohtani Y, Okamura S, Yoshida Y, Toyama K, Ejima Y. Surround suppression in the human visual cortex: an analysis using magnetoencephalography. *Vis Res.* 2002;42(15):1825–1835. doi:10.1016/S0042-6989(02)00103-7
25. Webb BS, Dhruv NT, Solomon SG, Tailby C, Lennie P. Early and late mechanisms of surround suppression in striate cortex of macaque. *J Neurosci.* 2005;25(50):11666–11675. doi:10.1523/JNEUROSCI.3414-05.2005
26. Martínez A, Anllo-Vento L, Sereno MI, et al. Involvement of striate and extrastriate visual cortical areas in spatial attention. *Nat Neurosci.* 1999;2(4):364–369. doi:10.1038/7274
27. Joo SJ, Boynton GM, Murray SO. Long-range, pattern-dependent contextual effects in early human visual cortex. *Curr Biol.* 2012;22(9):781–786. doi:10.1016/j.cub.2012.02.067
28. Joo SJ, Murray SO. Contextual effects in human visual cortex depend on surface structure. *J Neurophysiol.* 2014;111(9):1783–1791. doi:10.1152/jn.00671.2013
29. Di Russo F, Martínez A, Sereno MI, Pitzalis S, Hillyard SA. Cortical sources of the early components of the visual evoked potential. *Hum Brain Mapp.* 2002;15(2):95–111. doi:10.1002/hbm.10010
30. Vogel EK, Luck SJ. The visual N1 component as an index of a discrimination process. *Psychophysiology.* 2000;37(2):190–203. doi:10.1111/1469-8986.3720190
31. Schallmo MP, Murray SO. Identifying separate components of surround suppression. *J Vis.* 2016;16(1):2. doi:10.1167/16.1.2
32. Arroyo S, Lesser RP, Poon WT, Robert W, Webber S, Gordon B. Neuronal generators of visual evoked potentials in humans: visual processing in the human cortex. *Epilepsia.* 1997;38(5):600–610. doi:10.1111/j.1528-1157.1997.tb01146.x
33. Haynes JD, Roth G, Stadler M, Heinze HJ. Neuromagnetic correlates of perceived contrast in primary visual cortex. *J Neurophysiol.* 2003;89(5):2655–2666. doi:10.1152/jn.00820.2002
34. Butler PD, Silverstein SM, Dakin SC. Visual perception and its impairment in schizophrenia. *Biol Psychiatry.* 2008;64(1):40–47. doi:10.1016/j.biopsych.2008.03.023
35. Butler PD, Martinez A, Foxe JJ, et al. Subcortical visual dysfunction in schizophrenia drives secondary cortical impairments. *Brain.* 2007;130(2):417–430. doi:10.1093/brain/awl233
36. Hillyard SA, Vogel EK, Luck SJ. Sensory gain control (amplification) as a mechanism of selective attention: electrophysiological and neuroimaging evidence. *Philos Trans R Soc Lond B Biol Sci*. 1998;353(1373):1257–1270. https://www.ncbi.nlm.nih.gov/pmc/articles/PMC1692341/. Accessed July 25, 2023.
37. Bailey AJ, Gerst K, Finn PR. Intelligence moderates the relationship between delay discounting rate and problematic alcohol use. *Psychol Addict Behav*. 2020;34(1):175–181. doi:10.1037/adb0000471
38. Longenecker JM, Pokorny VJ, Kang SS, Olman CA, Sponheim SR. Self-reported perceptual aberrations in psychosis map to event-related potentials and semantic appraisals of objects. *J Abnorm Psychol.* 2021;130(7):785–796.
39. Yeap S, Kelly SP, Sehatpour P, et al. Visual sensory processing deficits in Schizophrenia and their relationship to disease state. *Eur Arch Psychiatry Clin Neurosc*. 2008;258(5):305–316. doi:10.1007/s00406-008-0802-2
40. Kayser J, Tenke CE. Principal components analysis of Laplacian waveforms as a generic method for identifying ERP generator patterns: I. Evaluation with auditory oddball tasks. *Clin Neurophysiol*. 2006;117(2):348–368. doi:10.1016/j.clinph.2005.08.034
41. Bruder G, Kayser J, Tenke C, et al. The time course of visuospatial processing deficits in schizophrenia: an event-related brain potential study. *J Abnorm Psychol.* 1998;107(3):399–411. doi:10.1037//0021-843x.107.3.399
42. McCourt ME, Shpaner M, Javitt DC, Foxe JJ. Hemispheric asymmetry and callosal integration of visuospatial attention in schizophrenia: a tachistoscopic line bisection study. *Schizophr Res.* 2008;102(1–3):189–196. doi:10.1016/j.schres.2008.03.021
43. Kayser J, Tenke CE. Hemifield-dependent N1 and event-related theta/delta oscillations: an unbiased comparison of surface Laplacian and common EEG reference choices. *Int J Psychophysiol.* 2015;97(3):258–270. doi:10.1016/j.ijpsycho.2014.12.011
44. Peirce JW. PsychoPy—psychophysics software in Python. *J Neurosci Methods.* 2007;162(1):8–13. doi:10.1016/j.jneumeth.2006.11.017
45. Wichmann FA, Hill NJ. The psychometric function: I. Fitting, sampling, and goodness of fit. *Percept Psychophys*. 2001;63(8):1293–1313. doi:10.3758/BF03194544
46. Kang SS, Lano TJ, Sponheim SR. Distortions in EEG interregional phase synchrony by spherical spline interpolation: causes and remedies. *Neuropsychiatr Electrophysiol*. 2015;1(1):9. doi:10.1186/s40810-015-0009-5
47. Tenke CE, Kayser J. Generator localization by current source density (CSD): implications of volume conduction and field closure at intracranial and scalp resolutions. *Clin Neurophysiol.* 2012;123(12):2328–2345. doi:10.1016/j.clinph.2012.06.005
48. Delorme A, Makeig S. EEGLAB: an open source toolbox for analysis of single-trial EEG dynamics including independent component analysis. *J Neurosci Methods.* 2004;134(1):9–21. doi:10.1016/j.jneumeth.2003.10.009
49. Vizioli L, Foreman K, Rousselet GA, Caldara R. Inverting faces elicits sensitivity to race on the N170 component: a cross-cultural study. *J Vis.* 2010;10(1):15. doi:10.1167/10.1.15
50. R Core Team. *R: A Language and Environment for Statistical Computing*. R Foundation for Statistical Computing; 2023. https://www.R-project.org/

51. Fox J. Diagnosing problems in linear and generalized linear models. In John Fox, Sanford Weisberg, eds. *An R Companion to Applied Regression*. 2nd ed. Boca Raton, FL: SAGE Publications; 2011.
52. Pinheiro J, Bates D; R Core Team. *Nlme: Linear and Nonlinear Mixed Effects Models.* 2023. https://CRAN.R-project.org/package=nlme. Accessed May 5, 2024.
53. Lenth RV. *Emmeans: Estimated Marginal Means, Aka Least-Squares Means.* 2023. https://CRAN.R-project.org/package=emmeans. Accessed May 5, 2024.
54. Benjamini Y, Hochberg Y. Controlling the false discovery rate: a practical and powerful approach to multiple testing. *J R Stat Soc Series B.* 1995;57(1):289–300. doi:10.1111/j.2517-6161.1995.tb02031.x
55. Celesia GG, Kaufman D, Cone S. Effects of age and sex on pattern electroretinograms and visual evoked potentials. *Electroencephalogr Clin Neurophysiol.* 1987;68(3):161–171. doi:10.1016/0168-5597(87)90023-2
56. Mitchell KW, Howe JW, Spencer SR. Visual evoked potentials in the older population: age and gender effects. *Clin Phys Physiol Meas.* 1987;8(4):317–324. doi:10.1088/0143-0815/8/4/004
57. Daffner KR, Haring AE, Alperin BR, Zhuravleva TY, Mott KK, Holcomb PJ. The impact of visual acuity on age-related differences in neural markers of early visual processing. *Neuroimage.* 2013;67:127–136. doi:10.1016/j.neuroimage.2012.10.089
58. William R. *Psych: Procedures for Psychological, Psychometric, and Personality Research*. Northwestern University; 2023. https://CRAN.R-project.org/package=psych
59. Silverstein SM. Visual perception disturbances in schizophrenia: a unified model. In: Spaulding WD, ed. *The Neuropsychopathology of Schizophrenia*. Nebraska Symposium on Motivation. Vol 63. Cham: Springer; 2016:77–132. doi:10.1007/978-3-319-30596-7_4
60. Longenecker JM, Krueger RF, Sponheim SR. Personality traits across the psychosis spectrum: a hierarchical taxonomy of psychopathology conceptualization of clinical symptomatology. *Pers Ment Health*. 2020;14(1):88–105. doi:10.1002/pmh.1448
61. Krueger RF, Derringer J, Markon KE, Watson D, Skodol AE. Initial construction of a maladaptive personality trait model and inventory for DSM-5. *Psychol Med.* 2012;42(9):1879–1890. doi:10.1017/S0033291711002674
62. Hetrick WP, Erickson MA, Smith DA. Phenomenological dimensions of sensory gating. *Schizophr Bull.* 2012;38(1):178–191. doi:10.1093/schbul/sbq054
63. Friedman T, Sehatpour P, Dias E, Perrin M, Javitt DC. Differential relationships of mismatch negativity and visual P1 deficits to premorbid characteristics and functional outcome in schizophrenia. *Biol Psychiatry.* 2012;71(6):521–529. doi:10.1016/j.biopsych.2011.10.037
64. Diamond A, Silverstein SM, Keane BP. Visual system assessment for predicting a transition to psychosis. *Transl Psychiatry.* 2022;12(1):1–9. doi:10.1038/s41398-022-02111-9
65. Strauss GP, Vertinski M, Vogel SJ, Ringdahl EN, Allen DN. Negative symptoms in bipolar disorder and schizophrenia: a psychometric evaluation of the brief negative symptom scale across diagnostic categories. *Schizophr Res.* 2016;170(2):285–289. doi:10.1016/j.schres.2015.12.014
66. Leeson VC, Barnes TRE, Hutton SB, Ron MA, Joyce EM. IQ as a predictor of functional outcome in schizophrenia: a longitudinal, four-year study of first-episode psychosis. *Schizophr Res.* 2009;107(1):55–60. doi:10.1016/j.schres.2008.08.014
67. Andreasen NC. The Scale for the Assessment of Negative Symptoms (SANS): conceptual and theoretical foundations. *Br J Psychiatry.* 1989;155(S7):49–52. doi:10.1192/S0007125000291496
68. DeRosse P, Karlsgodt KH. Examining the psychosis continuum. *Curr Behav Neurosci Rep*. 2015;2(2):80–89. doi:10.1007/s40473-015-0040-7
69. van Os J, Reininghaus U. Psychosis as a transdiagnostic and extended phenotype in the general population. *World Psychiatry*. 2016;15(2):118–124. doi:10.1002/wps.20310
70. Makin TR, Orban de Xivry JJ. Ten common statistical mistakes to watch out for when writing or reviewing a manuscript. Rodgers P, Parsons N, Holmes N, eds. *eLife*. 2019;8:e48175. doi:10.7554/eLife.48175
71. Saccenti E. What can go wrong when observations are not independently and identically distributed: a cautionary note on calculating correlations on combined data sets from different experiments or conditions. *Front Syst Biol*. 2023;3:1042156. doi:10.3389/fsysb.2023.1042156
72. Thiele A, Pooresmaeili A, Delicato LS, Herrero JL, Roelfsema PR. Additive effects of attention and stimulus contrast in primary visual cortex. *Cereb Cortex.* 2009;19(12):2970–2981. doi:10.1093/cercor/bhp070
73. Rodríguez-Álvarez MX, Durbán M, Eilers PHC, Lee DJ, Gonzalez F. Multidimensional adaptive P-splines with application to neurons' activity studies. *Biometrics.* 2023;79(3):1972–1985. doi:10.1111/biom.13755
74. Wood SN. *mgcv: Mixed GAM Computation Vehicle with Automatic Smoothness Estimation*. https://cran.r-project.org/package=mgcv. Accessed January 4, 2024.
75. Pedersen EJ, Miller DL, Simpson GL, Ross N. Hierarchical generalized additive models in ecology: an introduction with mgcv. *PeerJ.* 2019;7:e6876. doi:10.7717/peerj.6876
76. Wood SN. Low-rank scale-invariant tensor product smooths for generalized additive mixed models. *Biometrics.* 2006;62(4):1025–1036. doi:10.1111/j.1541-0420.2006.00574.x
77. Brehm L, Alday PM. Contrast coding choices in a decade of mixed models. *J Mem Lang*. 2022;125:104334. doi:10.1016/j.jml.2022.104334
78. Wood SN. *Generalized Additive Models: An Introduction with R*. 2nd ed. Boca Raton, FL: CRC Press/Taylor & Francis Group; 2017.
79. van Rij J, Hendriks P, van Rijn H, Baayen RH, Wood SN. Analyzing the time course of pupillometric data. *Trends Hear*. 2019;23:2331216519832483. doi:10.1177/2331216519832483
80. Wood SN, Pya N, Säfken B. Smoothing parameter and model selection for general smooth models. *J Am Stat Assoc.* 2016;111(516):1548–1563. doi:10.1080/01621459.2016.1180986
81. Marra G, Wood SN. Practical variable selection for generalized additive models. *Comput Stat Data Analysis*. 2011;55(7):2372–2387. doi:10.1016/j.csda.2011.02.004
82. Simpson G. *gratia: Graceful ggplot-Based Graphics and Other Functions for GAMs Fitted Using mgcv*. https://gavinsimpson.github.io/gratia/. Accessed January 4, 2024.
83. Ribolsi M, Lisi G, Di Lorenzo G, et al. Perceptual pseudoneglect in schizophrenia: candidate endophenotype and the role of the right parietal cortex. *Schizophr Bull.* 2013;39(3):601–607. doi:10.1093/schbul/sbs036
84. Klein SD, Olman CA, Sponheim SR. Perceptual mechanisms of visual hallucinations and illusions in psychosis. *J Psychiatr Brain Sci*. 2020;5:e200020. doi:10.20900/jpbs.20200020
85. Rokem A, Yoon J, Ooms R, Maddock R, Minzenberg M, Silver M. Broader visual orientation tuning in patients with

schizophrenia. *Front Hum Neurosci.* 2011;5:127. doi:10.3389/fnhum.2011.00127

86. Dias EC, Butler PD, Hoptman MJ, Javitt DC. Early sensory contributions to contextual encoding deficits in schizophrenia. *Arch Gen Psychiatry.* 2011;68(7):654–664. doi:10.1001/archgenpsychiatry.2011.17
87. Foxe JJ, Doniger GM, Javitt DC. Early visual processing deficits in schizophrenia: impaired P1 generation revealed by high-density electrical mapping. *Neuroreport.* 2001;12(17):3815–3820. http://journals.lww.com/neuroreport/Abstract/2001/12040/Early_visual_processing_deficits_in_schizophrenia_.43.aspx. Accessed August 19, 2020.
88. Sehatpour P, Dias EC, Butler PD, et al. Impaired visual object processing across an occipital-frontal-hippocampal brain network in schizophrenia: an integrated neuroimaging study. *Arch Gen Psychiatry.* 2010;67(8):772–782. doi:10.1001/archgenpsychiatry.2010.85
89. Phillips WA, Silverstein S. The coherent organization of mental life depends on mechanisms for context-sensitive gain-control that are impaired in schizophrenia. *Front Psychol.* 2013;4:37. doi:10.3389/fpsyg.2013.00307
90. Yeap S, Kelly SP, Sehatpour P, et al. Early visual sensory deficits as endophenotypes for schizophrenia: high-density electrical mapping in clinically unaffected first-degree relatives. *Arch Gen Psychiatry.* 2006;63(11):1180–1188. doi:10.1001/archpsyc.63.11.1180
91. Yeap S, Kelly SP, Reilly RB, Thakore JH, Foxe JJ. Visual sensory processing deficits in patients with bipolar disorder revealed through high-density electrical mapping. *J Psychiatry Neurosci.* 2009;34(6):459–464. https://www.ncbi.nlm.nih.gov/pmc/articles/PMC2783437/. Accessed March 25, 2023.
92. Handy TC, Khoe W. Attention and sensory gain control: a peripheral visual process? *J Cogn Neurosci.* 2005;17(12):1936–1949. doi:10.1162/089892905775008715
93. Luck SJ, Woodman GF, Vogel EK. Event-related potential studies of attention. *Trends Cogn Sci.* 2000;4(11):432–440. doi:10.1016/s1364-6613(00)01545-x
94. Yang E, Tadin D, Glasser DM, Wook Hong S, Blake R, Park S. Visual context processing in bipolar disorder: a comparison with schizophrenia. *Front Psychol.* 2013;4:569. doi:10.3389/fpsyg.2013.00569
95. Ventura J, Hellemann GS, Thames AD, Koellner V, Nuechterlein KH. Symptoms as mediators of the relationship between neurocognition and functional outcome in schizophrenia: a meta-analysis. *Schizophr Res.* 2009;113(2):189–199. doi:10.1016/j.schres.2009.03.035
96. Flevaris AV, Murray SO. Attention determines contextual enhancement versus suppression in human primary visual cortex. *J Neurosci.* 2015;35(35):12273–12280. doi:10.1523/JNEUROSCI.1409-15.2015
97. Ramalingam N, McManus JNJ, Li W, Gilbert CD. Top-down modulation of lateral interactions in visual cortex. *J Neurosci.* 2013;33(5):1773–1789. doi:10.1523/JNEUROSCI.3825-12.2013
98. Klein SD, Shekels LL, McGuire KA, Sponheim SR. Neural anomalies during vigilance in schizophrenia: diagnostic specificity and genetic associations. *Neuroimage Clin.* 2020;28:102414. doi:10.1016/j.nicl.2020.102414
99. Schallmo MP, Sponheim SR, Olman CA. Abnormal contextual modulation of visual contour detection in patients with schizophrenia. Herzog MH, ed. *PLoS One.* 2013;8(6):e68090. doi:10.1371/journal.pone.0068090
100. Pokorny VJ, Lano TJ, Schallmo MP, Olman CA, Sponheim SR. Reduced influence of perceptual context in schizophrenia: behavioral and neurophysiological evidence. *Psychol Med.* 2019;51:786–794. doi:10.1017/S0033291719003751
101. Gruzelier JH. Functional neuropsychophysiological asymmetry in schizophrenia: a review and reorientation. *Schizophr Bull.* 1999;25(1):91–120. doi:10.1093/oxfordjournals.schbul.a033370
102. Christie J, Ginsberg JP, Steedman J, Fridriksson J, Bonilha L, Rorden C. Global versus local processing: seeing the left side of the forest and the right side of the trees. *Front Hum Neurosci.* 2012;6:28. doi:10.3389/fnhum.2012.00028
103. Han S, Weaver JA, Murray SO, Kang X, Yund EW, Woods DL. Hemispheric asymmetry in global/local processing: effects of stimulus position and spatial frequency. *Neuroimage.* 2002;17(3):1290–1299. doi:10.1006/nimg.2002.1255
104. Barnett KJ, Kirk IJ, Corballis MC. Right hemispheric dysfunction in schizophrenia. *Laterality*. 2005;10(1):29–35. doi:10.1080/13576500442000175
105. David AS, Cutting JC, eds. *The Neuropsychology Of Schizophrenia*. Hillsdale, NJ: Lawrence Erlbaum Associates; 1994:231–242.
106. Rotenberg VS. An integrative psychophysiological approach to brain hemisphere functions in schizophrenia. *Neurosci Biobehav Rev.* 1994;18(4):487–495. doi:10.1016/0149-7634(94)90003-5
107. Lindell AK. On the interrelation between reduced lateralization, schizotypy, and creativity. *Front Psychol.* 2014;5:813. doi:10.3389/fpsyg.2014.00813
108. Schmitz J, Fraenz C, Schlüter C, et al. Schizotypy and altered hemispheric asymmetries: the role of cilia genes. *Psychiatry Res Neuroimaging*. 2019;294:110991. doi:10.1016/j.pscychresns.2019.110991
109. Gurin L, Blum S. Delusions and the right hemisphere: a review of the case for the right hemisphere as a mediator of reality-based belief. *J Neuropsychiatry Clin Neurosci.* 2017;29(3):225–235. doi:10.1176/appi.neuropsych.16060118
110. Michele R, Giacomo K, Valentina M, et al. Abnormal brain lateralization and connectivity in Schizophrenia. *Rev Neurosci.* 2009;20(1):61–70. doi:10.1515/REVNEURO.2009.20.1.61
111. Mengotti P, Käsbauer AS, Fink GR, Vossel S. Lateralization, functional specialization, and dysfunction of attentional networks. *Cortex.* 2020;132:206–222. doi:10.1016/j.cortex.2020.08.022
112. Barnett K, Kirk I, Corballis M. Right hemispheric dysfunction in schizophrenia. *Laterality*. 2005;10(1):29–35. doi:10.1080/13576500442000175
113. Shapley RM, Xing D. Local circuit inhibition in the cerebral cortex as the source of gain control and untuned suppression. *Neural Netw*. 2013;37:172–181. doi:10.1016/j.neunet.2012.09.005
114. Katzner S, Busse L, Carandini M. GABAA inhibition controls response gain in visual cortex. *J Neurosci.* 2011;31(16):5931–5941. doi:10.1523/JNEUROSCI.5753-10.2011
115. Yoon JH, Maddock RJ, Rokem A, et al. GABA concentration is reduced in visual cortex in schizophrenia and correlates with orientation-specific surround suppression. *J Neurosci.* 2010;30(10):3777–3781. doi:10.1523/JNEUROSCI.6158-09.2010
116. Yoon JH, Maddock RJ, Cui ED, et al. Reduced in vivo visual cortex GABA in schizophrenia, a replication in a recent onset sample. *Schizophr Res.* 2020;215:217–222. doi:10.1016/j.schres.2019.10.025
117. Uhlhaas PJ. Dysconnectivity, large-scale networks and neuronal dynamics in schizophrenia. *Curr Opin Neurobiol.* 2013;23(2):283–290. doi:10.1016/j.conb.2012.11.004

118. Hipp JF, Engel AK, Siegel M. Oscillatory synchronization in large-scale cortical networks predicts perception. *Neuron.* 2011;69(2):387–396. doi:10.1016/j.neuron.2010.12.027
119. Sauer A, Grent-'t-Jong T, Wibral M, Grube M, Singer W, Uhlhaas PJ. A MEG Study of visual repetition priming in schizophrenia: evidence for impaired high-frequency oscillations and event-related fields in thalamo-occipital cortices. *Front Psychiatry.* 2020;11:561973. doi:10.3389/fpsyt.2020.561973
120. Ramsay IS, Lynn PA, Schermitzler B, Sponheim SR. Individual alpha peak frequency is slower in schizophrenia and related to deficits in visual perception and cognition. *Sci Rep.* 2021;11(1):17852. doi:10.1038/s41598-021-97303-6
121. Ramsay IS, Pokorny VJ, Lynn PA, Klein SD, Sponheim SR. Limited consistency and strength of neural oscillations during sustained visual attention in schizophrenia. *Biol Psychiatry*. 2023;9:337–345. doi:10.1016/j.bpsc.2023.02.001
122. Sponheim SR, Stim JJ, Engel SA, Pokorny VJ. Slowed alpha oscillations and percept formation in psychotic psychopathology. *Front Psychol.* 2023;14:1144107. doi:10.3389/fpsyg.2023.1144107
123. O'Connell RG, Schneider D, Hester R, Mattingley JB, Bellgrove MA. Attentional load asymmetrically affects early electrophysiological indices of visual orienting. *Cereb Cortex*. 2011;21(5):1056–1065. doi:10.1093/cercor/bhq178
124. Bagherzadeh Y, Baldauf D, Pantazis D, Desimone R. Alpha synchrony and the neurofeedback control of spatial attention. *Neuron.* 2020;105(3):577–587.e5. doi:10.1016/j.neuron.2019.11.001
125. Shaw AD, Knight L, Freeman TCA, et al. Oscillatory, computational, and behavioral evidence for impaired GABAergic inhibition in schizophrenia. *Schizophr Bull.* 2020;46(2):345–353. doi:10.1093/schbul/sbz066
126. Nakazawa K, Zsiros V, Jiang Z, et al. GABAergic interneuron origin of schizophrenia pathophysiology. *Neuropharmacology.* 2012;62(3):1574–1583. doi:10.1016/j.neuropharm.2011.01.022
127. Jahshan C, Wynn JK, McCleery A, Glahn DC, Altshuler LL, Green MF. Cross-diagnostic comparison of visual processing in bipolar disorder and schizophrenia. *J Psychiatr Res.* 2014;51:42–48. doi:10.1016/j.jpsychires.2013.12.014
128. Pokorny VJ, Lano TJ, Schallmo MP, Olman CA, Sponheim SR. Reduced influence of perceptual context in schizophrenia: behavioral and neurophysiological evidence. *Psychol Med.* 2021;51(5):786–794. doi:10.1017/S0033291719003751